frontiers in Materials

ORIGINAL RESEARCH
published: 13 November 2020
doi: 10.3389/fmats.2020.504642

Progress in Silk Fibroin Based Composite Scaffold/Hydrogel: Silk Fibroin/PEG Hydrogel for the RPE Regeneration a Promising Biomaterial for Clinical Application

*Yong Woon Jeong, Han Sol Kim, Muthukumar Thangavelu, Min Joung Choi, Gi Won Lee, Cheol Ui Song, Jeong Eun Song and Gilson Khang**

Department of BIN Convergence Technology, Polymer Nano Science & Technology, Polymer Materials Fusion Center, Jeonbuk National University, Jeonju, South Korea

OPEN ACCESS

Edited by:
Nicola Maria Pugno, University of Trento, Italy

Reviewed by:
Pasquale Vena, Politecnico di Milano, Italy
Domenico De Tommasi, Politecnico di Bari, Italy

***Correspondence:**
Gilson Khang
gskhang@jbnu.ac.kr

Specialty section:
This article was submitted to Mechanics of Materials, a section of the journal Frontiers in Materials

Received: *14 October 2019*
Accepted: *13 August 2020*
Published: *13 November 2020*

Citation:
Jeong YW, Kim HS, Thangavelu M, Choi MJ, Lee GW, Song CU, Song JE and Khang G (2020) Progress in Silk Fibroin Based Composite Scaffold/Hydrogel: Silk Fibroin/PEG Hydrogel for the RPE Regeneration a Promising Biomaterial for Clinical Application. Front. Mater. 7:504642. doi: 10.3389/fmats.2020.504642

Retinal pigment epithelium (RPE) plays a decisive role in the normal function of the retina, especially in the maintenance of photoreceptors. RPE dysfunction, loss of sight, and degeneration has been implicated as the cause of many retinal diseases including pigmented retinitis and age-related macular degeneration (AMD). Silk fibroin (SF) is a biodegradable natural polymer with biocompatibility, non-toxic, and non-immunological properties. In this study, hydrogel material was prepared by mixing it with PEG [poly (ethylene glycol)] a synthetic polymer. SF hydrogel (SH) and with PEG (SPH) were prepared with different sonication times. The SH and SPH were prepared with different sonication time (20s SH, 30s SH, 20s SPH, and 30s SPH were prepared, respectively. The prepared SH and SPH were physio chemically characterized by SEM, FTIR, compressive strength, porosity, and *in vitro* biocompatibility were analyzed using MTT assay along with cell adhesion and cell proliferation, their gene expression was analyzed using RT-PCR. As a result, the 20s SPH hydrogel exhibited superior biocompatibility, cell adhesion, and improved cell growth compared to pure SH. Their respective genes expression for retinal function and matrix production was also positively influenced by 20s SPH with an increase in gene expression folds of RPE65, CRALBP. The obtained results suggest that the 20s SPH hydrogel can be used as an alternative material for the application of retinal regeneration and delivery.

Keywords: silk fibroin, polyethylene glycol, retinal pigment epithelial, hydrogel, gene expression, porosity

INTRODUCTION

Retinal pigment epithelial cells (RPE) are the outermost layer of retina consisting of ten layers (Hageman et al., 2001). RPE cells nourish the retinal visual cells and are firmly attached to the choroid and retinal visual cells. RPE is composed of a single layer of hexagonal cells with dense pigment granules characterized by a dark color with melanin pigment (Bok, 1993; Strauss, 2005, 2009). RPE has several functions and plays an important role in maintaining the normal visual function of the retina (Simo et al., 2010). Degeneration of the RPE causes various retinal diseases.

Diseases of retinal and retinal functions can lead to permanent loss of visual function without any definitive treatment. The adverse effects of quality of life and poor vision on daily living activities affect the entire age range. Age-related macular degeneration (AMD) is a major cause of blindness and that cannot be reversed (Bressler et al., 1988; Liang and Godley, 2003). In the United States, there are 200,000 new cases a year. Death or malfunction of irreversible photoreceptors is common to all these pathologies. The rate of visual loss due to retinal degeneration is expected to increase due to aging. Currently, there was a lack of a cure for this, and studies are carried out to make a suitable scaffold that supports cell transplantation (Mandelcorn et al., 1975; Algvere et al., 1997; Lu et al., 2009; Bhutto and Lutty, 2012).

Natural polymers that can be used as a substrates for RPE regeneration including collagen, alginate, hyaluronic acid, gellan gum, gelatin, and silk fibroin (SF) and synthetic polymers including PLGA, PCL, and PEG (Lee et al., 2017; Wang and Han, 2017; Park et al., 2018; Kim et al., 2019; Shin et al., 2019). As a carrier that delivers RPE cells, it should have good cell adhesion, survival rate, invasiveness and biocompatible properties that helps in binding to other tissues of the retina. In addition, to increase cell efficiency, it should be an injectable and biodegradable material (Santin et al., 1999; Vepari and Kaplan, 2007; Binder, 2011). Among them, SF occupies 70–80% that is an excellent biomaterial with better mechanical, excellent water, and oxygen permeability properties; it is also used as a support material for cell adhesion, proliferation, and expression of the extracellular matrix (Wang et al., 2008; Yucel et al., 2009; Chao et al., 2010). PEG is a hydrophilic polymer having long linear chains and does not interact with biological chemicals. Therefore, PEG is widely used in medical instruments and materials for improving its physical properties (Zustiak and Leach, 2010; Kim et al., 2019).

Therefore, in this study, SH and SPH hydrogels were prepared and optimized to evaluate the suitability of new hydrogels for RPE cell regeneration. 4% SF and SFH were prepared by sonicating for the 20s and 30s, respectively. Porosity, biodegradability, FT-IR, and hygroscopicity were measured to characterize the hydrogel physiochemical properties. Cell attachment and proliferation rate of RPE cells were confirmed using MTT assay.

MATERIALS AND METHODS

Materials

Bombyx mori was purchased from Kyebong Farm (Korea) and polyethylene glycol (MW 10,000, Sigma-Aldrich) and Trizol (Invitrogen, Life Technologies Co, Groningen, Netherlands) were used in this study. The reagents required for cell culture were purchased from Gibco (United States), all other chemicals and organic solvents used were of HPLC grade.

Silk Fibroin Extract

The cocoon was cut into 1 cm × 1 cm pieces and SF solution was prepared by removing the sericin from the cocoons, by boiling them in 0.02 M sodium carbonate solution (Na_2CO_3, Showa chemical, Japan) for a minimum of 30 min and rinsed five times with double distilled water (dDW). The purified SF was dissolved in a 9.3 M lithium bromide (LiBr, Kanto Chemical, Japan) solution at 60°C for around 4 h. The obtained SF solution was dialyzed using a cellulose dialysis membrane (Snakeskin® Dialysis Tubing, 3.5K Mw, Thermo science, United States) in distilled water for 48 h. During the dialysis, the distilled water was replaced frequently, and the dialyzed aqueous solution was filtered and stored in the refrigerator until further use. The final concentration of the SF aqueous solution was concentrated to 8%.

Preparation of Silk Fibroin/PEG Hydrogel

For the preparation of SPH, PEG (10% v/v) was dissolved in distilled water and they were slowly added to the aqueous solution of SF and finally diluted to 4%. For the preparation of SH and SPH, the aqueous solution was added to the vial and tip sonication was performed for a period of 20s and 30s separately for each batch. 1ml of each solution was dispensed into a 24-well plate and stored in the refrigerator until further use (Samal et al., 2013). The hydrogel for the physicochemical characterization was prepared by lyophilization (using freeze dry method) by pouring them in a 15 mm diameter petri dish, followed by refrigerating, freezing for 4 h and quenching at −80°C, finally, they were lyophilized and stored for further use. The material sizes of 8 mm were cut using a biopsy.

Surface Morphology and Pore Size

Scanning electron microscopy (SEM, Hitachi Co, Model S-2250N, Japan) was performed to confirm the surface morphology and porosity of 20s and 30s SH and SPH samples. Plasma-palladium coating was performed using a plasma sputter (Emscope, Model SC500K, United Kingdom) under argon gas. The samples ware observed at an accelerating voltage of 1.5 kV. To measure the pore size of each scaffold, image J program tools were used by taking the cross-sectional images and calculating their average pore size.

Change in the Functional Group Using FTIR

The change in the functional group of SF aqueous solution, PEG powder, and prepared hydrogels was confirmed by FT-IR analyzed using ATR mode with the lyophilized samples (FT-IR Spectroscopy- FT-IR, GX, Perkin Elmer, Connecticut, United States). All the spectrums were observed between 4,000 and 400 cm^{-1} at a resolution of 4 cm^{-1} with a minimum of 50 scans.

Compressing Test Properties of the Hydrogel

A universal physical property meter (TMS-Pro, Food Technology Corporation, Sterling, United States) was used to measure the compressive strength of the prepared hydrogels in compressive mode at a constant speed of 5 mm/min and the measurement distance was set to be 3 mm. The as prepared hydrogels are cut into cylindrical shape with the height 50 mm. The analysis was carried out at 25°C and the test are repeated at least 5 times for each samples.

Porosity of the Prepared Hydrogel

The porosity of the prepared hydrogels was evaluated by the principle of Archimedes via fluid displacement measurement technique. Before the analysis, the test sample was immersed in the known volume of distilled water (V_1) for 10 min. The total volume of distilled water containing the scaffold after 10 min was referred to as V_2. The hydrated scaffold was removed and the remaining volume of distilled water was recorded as (V_3). The porosity of the scaffold was estimated by using the following equation with the average of 4 measurements.

$$\text{Porosity } (\%) = \frac{V_1 - V_3}{V_2 - V_3} \times 100$$

Degradation of the Hydrogel

Freeze-dried hydrogel scaffold (W_f) was immersed in 1M phosphate-buffered saline (PBS, pH 7.4) and their percentage of weight loss was analyzed on 7, 14, 21, and 28 days over time. Briefly, the scaffold was immersed in PBS and incubated at 37 ± 0.5°C, after specific time intervals the PBS was carefully removed and the scaffolds are dried and their weight (W_d) was measured after 7, 14, 21, and 28 days. PBS was changed every day (n = 3). The degradability was calculated using the following equation.

$$\textit{Degradation}\,(\%) = \frac{W_f - W_d}{W_f} \times 100$$

Isolation and Culturing of RPE Cells

All the animal experiments were performed in accordance with the guidelines and the approval of the Jeonbuk National University Animal Care Committee (CBNUACC), Jeonju, South Korea. The protocol was approved by the CBNUACC. The RPE cells were isolated from a 3 weeks old female New Zealand white rabbit (Hanil laboratory animal center, Wanju, South Korea). The eyes of the rabbits were harvested using sterile surgical scissors and unwanted surrounding tissues (anterior eye and vitreous body were removed) were removed, washed several times with PBS, and stored in PBS. For RPE isolation the specimen was incubated in 0.2% collagenase A (Roche Diagnostics, Germany) for 60 min followed by filtering using 70 μm filter, and the content were centrifuged at 15,000 rpm for 5 min. The cell pellets were suspended using 1 mL RPE medium (DMEM/F-12 (Dulbecco's Modified Eagle's Media, Gibco, United States)/Ml streptomycin, Gibco) adding FBS (Gibco) with 1% penicillin-streptomycin (PS, 100 units/mL penicillin and 100 μg/mL penicillin-streptomycin) in a cell culture dish. The cells were placed inside the incubator at 37°C in 5% CO_2, and the culture medium was changed every 2 days until it reaches as confluency. After that, the cells (2×10^5 cells) were seeded on the surface of the hydrogel and each well was filled with medium after seeding the cells for 30 min and incubated at 37°C in 5% CO_2. The culture medium was changed every 2 days until the specified time intervals.

Initial Attachment and Proliferation of RPE Cell

In order to confirm the initial adhesion of the retinal pigment epithelial cells, 1×10^5 cells were seeded on each hydrogel and cultured in an incubator for 30 min. After that, the culture solution was removed, and 2.5% glutaraldehyde was added, and the cells were fixed by refrigerated storage for 24 h. Nuclei were then stained with UltraCruz™ Mounting Medium (Santa Cruz, United States) and photomicrographs were taken using a fluorescence microscope (Eclipse TE 2000-U, Nikon, Japan) to determine cell density per square mm^2. The photographed images were quantified using the Image J program.

Biocompatibility of the Hydrogels Using MTT

Biocompatibility of the prepared SF and SF/P hydrogels were analyzed using MTT (dimethylthiazol-2-yl-2,5-diphenyltetrazolium bromide) assay to determine cell viability on each hydrogel. 2×10^5 RPE cells were seeded on each hydrogel and filled with the media, after respective time point the media was removed and they were treated with 0.1 mL of MTT solution (50 μg/mL) each on day 1, 3, 7, and 14 of the experimental period and kept in an incubator for 3 h at 37°C in 5% CO_2. After the incubation period, 1 mL of dimethylsulfoxide (DMSO, Sigma, United States) was added to completely dissolve the purple crystals, then the solution was dispensed into fresh 96-well plates and absorbance was measured at 570 nm.

Reverse Transcription-Polymers Chain Reaction (RT-PCR)

In order to confirm the specific gene expression level of RPE cells seeded on SF and SF/P hydrogel, RT-PCR was performed on 7 day cultured cells on the hydrogel. RNA was extracted from RPE cells by centrifugation at 12,000 rpm for 15 min at 4°C using 1 mL of trizol (Invitrogen™ Life Technologies Co., Groningen, Netherlands) and 0.2 mL of chloroform (Sigma, United States). The expression of mRNA in the sample was confirmed by RPE-specific 65 kDa (RPE65), natriuretic peptide-A receptor (NPRA), and cellular retinaldehyde -binding protein (CRALBP) markers. All samples were denatured at 95°C for 30 s followed by annealing at a specific temperature of the primer and amplified at 72°C for 1 min/kb to synthesize complementary DNA (cDNAs). The expression were confirmed by running the samples through the electrophoretic gel and imaged at 360 nm using an ultraviolet-transilluminator tester (Flourchem® HD2, Alpha Innotech, San Leandro, United States). The images were quantified using the Image J program. The primers used in this study are listed in **Table 1**.

Statistical Analysis

Data are presented as means ± SD (SD), n = 3. Statistical analysis of each experiment was considered to be significant when

TABLE 1 | The primer for β-actin, RPE65, NPR-A, and CRALBP mRNA.

Gene		Primer sequences
β-actin	F	5′-GCCATCCTGCTCCGTCTGGACCTGGCT-3′
	R	5′-GTGATGACCTGGCCGTCAGGCAGC-3′
RPE65	F	5′-GCCCTCCTGCACAAGTTTGACTTT-3′
	R	5′-AGTTGGTCTCTGTGCAAGCGTAGT-3′
NPRA	F	5′-GTTGAGCCCAGTAGCCTTGAG-3′
	R	5′-CCCAAGGAGCCAGTAGGTCCG-3′
CRALBP	F	5′-TTCCGCATGGTACCTGAAGAGGAA-3′
	R	5′-ACTGCAGCCGGAAATTCACATAGC-3′

$^{*}p < 0.5$, $^{**}p < 0.05$, and $^{***}p < 0.01$ by Student's *t*-test (Excel 2013, Microsoft).

RESULTS AND DISCUSSION

Surface Morphology of the Hydrogel Scaffold

Surface morphology along with the pore size, shape, and thickness of the interconnecting pore walls of the prepared freeze-dried SF/SPH hydrogels was observed using SEM. It was confirmed that the SF/SPH hydrogel had a relatively small pore size in all groups, and the pore size was observed to be decreasing as the PEG content increases. As mentioned above, increasing the sonication time of the hydrogels results in the decrease of the pore size due to the formation of smaller molecules, smaller crystal structure, and smaller pore size as mentioned in **Figure 1**.

Change in Functional Group Analyses Using FT-IR

The change in the functional group analysis of the prepared SF, PEG, and SH/SPH hydrogels was carried out using FT-IR for qualitative analysis in the range of 4,000 ∼ 400 cm^{-1}. The results were shown in **Figure 2A**. FT-IR analysis results of SF and SPH showed the characteristic amide I, II, and III peaks at 1,621, 1,515, and 1,231 cm^{-1}, respectively. The characteristic peak of -OH was observed at 2900–3,300 cm^{-1}, and the characteristic peak of PEG -CH was observed at 2880 cm^{-1}, and the peak of -COC-group was observed at 1101 cm^{-1} (Ohno et al., 1992). It was observed that the sonication time of SH and SPH did not change the functional properties or structural change of the hydrogels, indicating that the chemical structure of SF and SPH did not change during the preparation process. In addition, SPH was confirmed to show a physical bond, not a chemical bond, when the PEG was mixed with SF. The peak intensity and respective peaks of SF did not change during the whole sonication process.

Compressive Strength of the Hydrogels

Compressive strength was measured to evaluate the physical properties of the 20s and 30s sonicated SF and SF/P hydrogels. The compressive strength values of the 20s, 30s SF, and SF/P hydrogels were observed to be 19.71 ± 0.28, 21.62 ± 0.56, 20.65 ± 0.78, and 22.5 ± 0.13 MPa, respectively. The obtained results clearly confirm that increasing the sonication time of the hydrogels increases its compressive strength due to the increase in the viscosity of the SF due to the addition of PEG. This change in the compressive strength of the SF material is due to

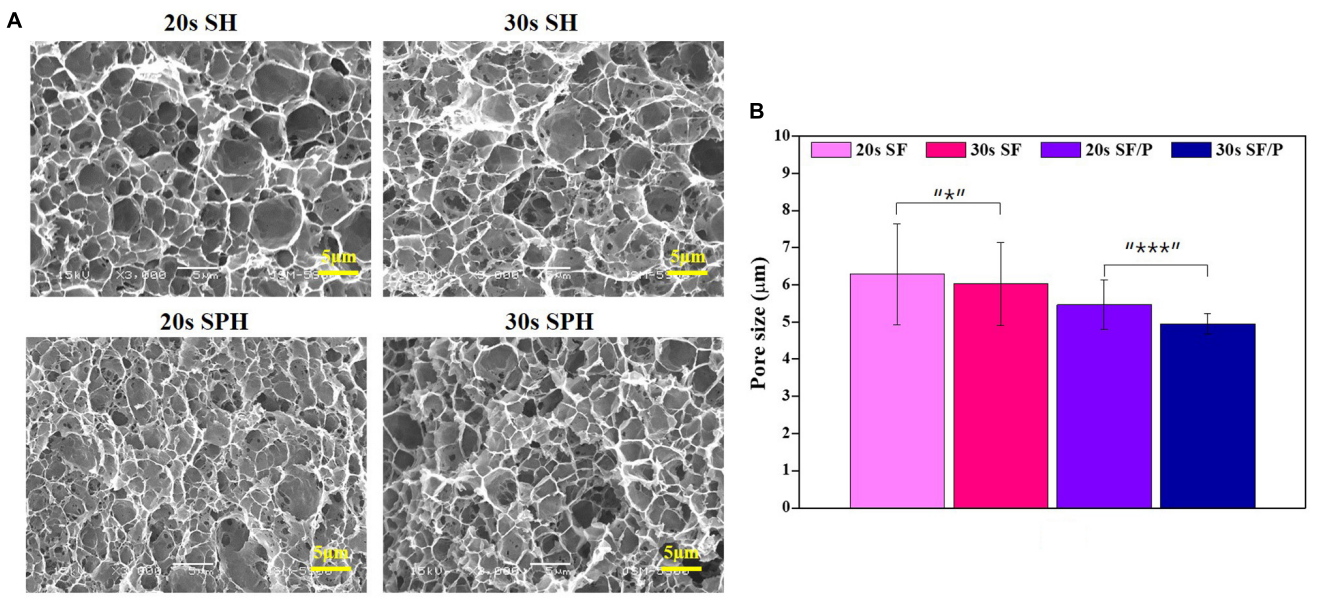

FIGURE 1 | (A) SEM microphotographs to insert gross image of SF, SF/P hydrogels (magnification with 3,000×, scale bar = 5 μm). **(B)** Pore size of freeze dried SF and SF/P hydrogels ($n = 3$ in each group; $^{*}p < 0.05$ and $^{***}p < 0.001$).

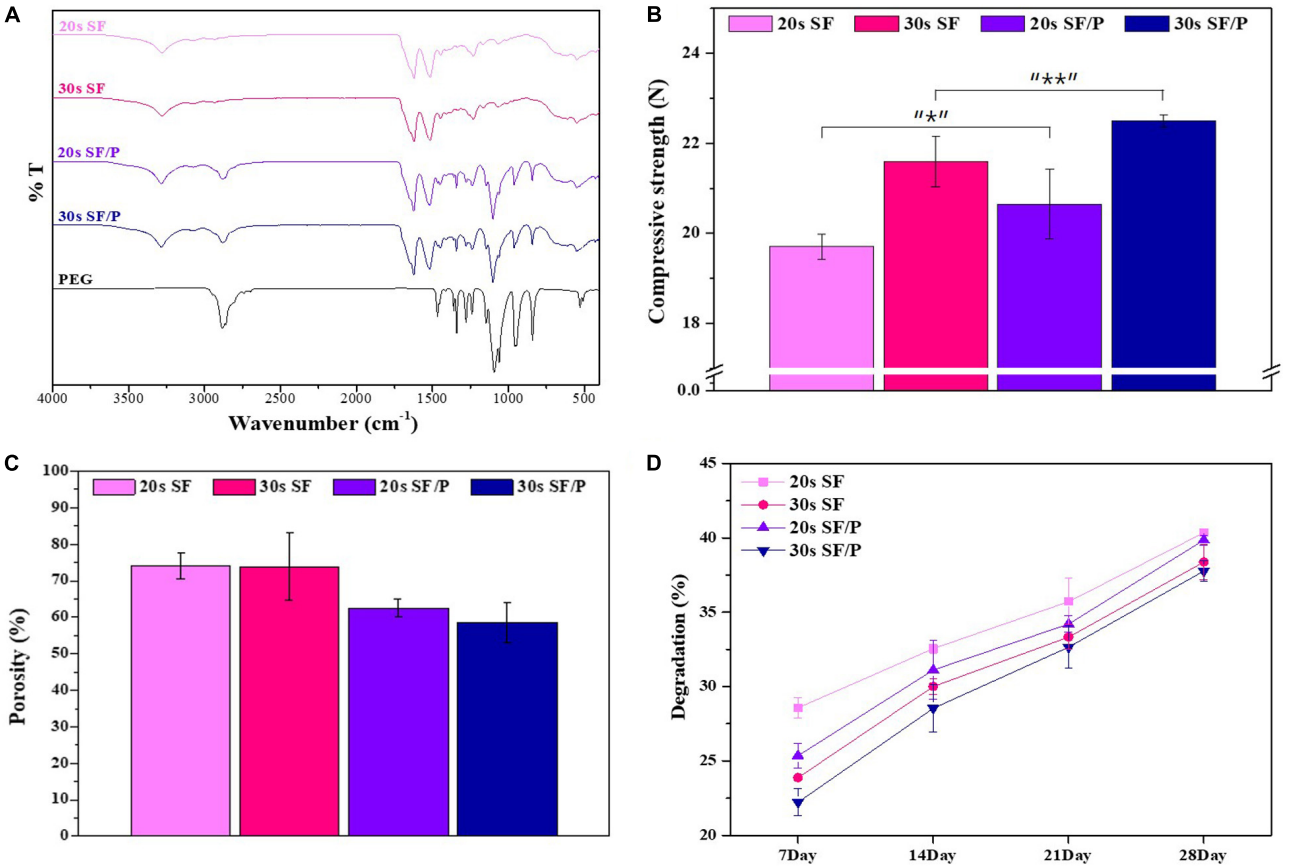

FIGURE 2 | (A) FT-IR spectra of SF, SF/P hydrogels, and PEG powder. Graphs showing **(B)** compressive strength, **(C)** porosity, and **(D)** degradation test of 20s SF, 30s SF, 20s SF/P, and 30s SF/P hydrogels ($n = 3$; *$p < 0.5$, **$p < 0.05$, and ***$p < 0.01$).

changing the viscosity of the final hydrogel along with the sonication time.

Porosity Measurements of Hydrogels

The porosity characteristic properties of the material are crucial for hydrogel scaffold because it helps in cell adhesion, penetration, proliferation, and nutrient and oxygen exchange (Li et al., 1996). The obtained results of the prepared SF and SF/P hydrogel sonicated for the 20s and 30s results were shown in **Figure 2B**. The 20s SF/P hydrogel showed more than 60% porosity compare to other studied hydrogels including 20s SF, 30s SF, and 30s SF/P, and the results were similar to the pore size (**Figure 2C**). The results show that the addition of PEG results in increased viscosity that results in decreased porosity, and reduced pore size with increasing the sonication time. As a result, the size of the pores is generated by the size of the ice crystals, and thus it is confirmed that the friendliness is formed by combining with PEG to form smaller pores.

Degradation Properties of Hydrogels

The degradation rate was evaluated to confirm the biodegradability of the prepared SF and SPH hydrogel. Hydrogels are problematic even if they are not degraded quickly or decomposed. Therefore, hydrogels should provide adequate biodegradability property for RPE cell proliferation (Sung et al., 2004; Lu et al., 2011). The results show that the degradation rate of SF, SPH hydrogel for 28 days are shown in **Figure 2D**. Similar degradation rates were observed in all groups and 20s hydrogel degradation occurred well. This is because the shorter the time of the sonication, the lesser the binding of the hydrogel, and the higher the porosity, as shown in **Figure 2B**.

Initial Attachment and Proliferation of RPE Cells

In order to evaluate the initial cell adhesion and proliferation and viability percentage rate of the 20s and 30s sonicated SF and SF/P hydrogel were analyzed using MTT assay and nuclear stain, by culturing RPE cells on the surface of the material. The initial adhesions of the cells are affected by the surface roughness and hydrophilicity of the material (Hallab et al., 2001; Chanasakulniyom et al., 2015). The higher the rate of adhesion, the shorter the cell diffusion time, which helps in the increased cell proliferation. The initial cell adhesion on the surface of the 20s, 30s SF, and SF/P hydrogels after 30 min of sowing were calculated to be 619 ± 39.11, 587 ± 35.32, 680 ± 27.29, and 631 ± 61.33 cell/mm^2, respectively, that were calculated from

the respective images from **Figure 3**. The initial cell adhesion was significantly ($p < 0.05$) increased in the 20s SF/P hydrogels compared with other hydrogels. The cell viability was analyzed using MTT assay studied on 1, 3, 7, and 14 days on the 20s, 30s SF, and SF/P hydrogels (**Figure 4A**). Initial cell viability rate on day 1 and 3 were observed to be same whereas, the proliferation and viability of the RPE cells were observed to be significantly increased on all the samples/When compared between the samples studied, it was confirmed that 20s SF/P hydrogel had significantly increased ($p < 0.05$) cell proliferation rate compared with 20s and 30s SF hydrogel group. Moreover, the cell viability was observed to significantly increased on days 7 and 14 in the 20s SF/P hydrogel followed by 30s SF/P which is due to the addition of PEG that resulted in their decreased porosity and well-interconnected walls compared to 20s and 30s SF samples. This result clearly confirms that the material physical property and their porosity play an evident role in the increased cell adhesion.

Gene Expressions in Hydrogels Using RT-PCR

The effect of prepared 20s and 30s SF and SF/P hydrogels were evaluated for its ability to support RPE cell growth by studying mRNA expression taking RPE related gene marker genes. *In vitro*, RPE cells were cultured on the 20s and 30s SF and SF/P hydrogels for a period of 1, 3, and 7 days, followed by RNA isolation and RT-PCR to confirm specific gene expressions (Liao et al., 2010). Based on the overall genetic marker Beta-actin, RPE65 provides guidelines for making proteins essential

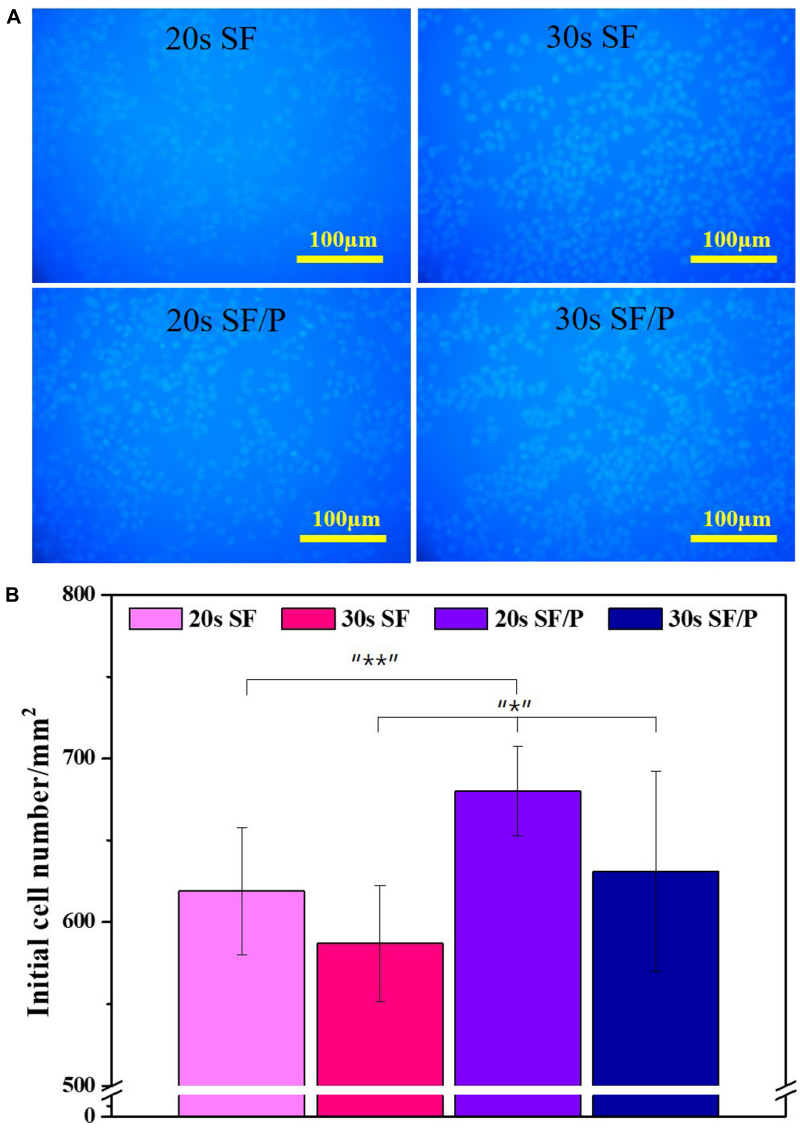

FIGURE 3 | (A) Initial attachment Nuclear stain photograph, **(B)** initial attachment cell number graph on SF and SF/P hydrogels (Magnification is 200×; scale bar = 100 µm; $n = 3$ in each group; $^{*}p < 0.5$, $^{**}p < 0.05$, and $^{***}p < 0.01$).

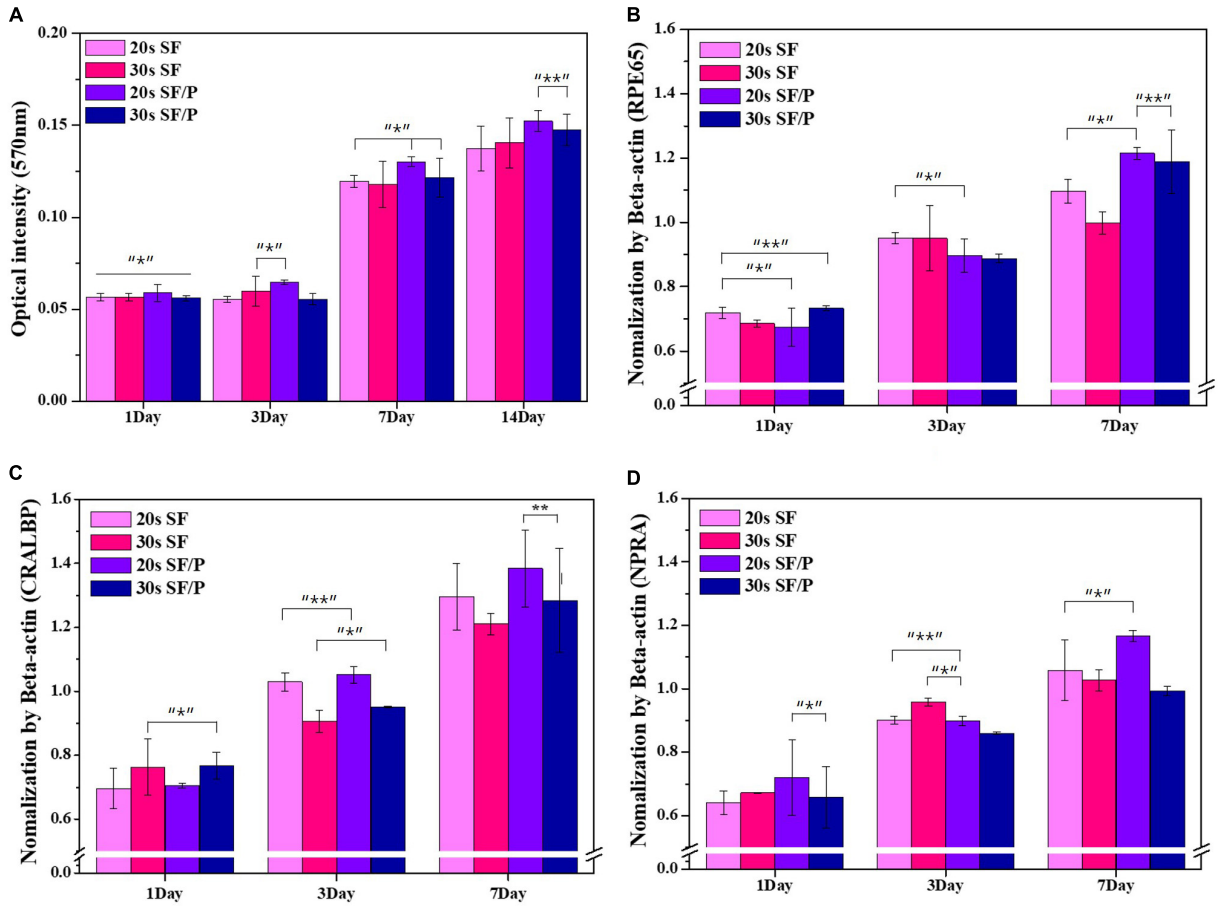

FIGURE 4 | (A) Cell proliferation result by MTT assay of RPE cell on SF and SF/P hydrogels ($n = 3$ in each group; $^{*}P < 0.05$, $^{**}P < 0.01$). Gene expression of RPE on SF/P hydrogels was analyzed by RT-PCR after 1, 3, and 7 days. Quantitative analysis of RPE65 **(B)**, NRPA **(C)**, and CRALBP **(D)** by normalization of ß-actin ($n = 3$; $^{*}p < 0.5$, $^{**}p < 0.05$, and $^{***}p < 0.01$).

for normal vision, produced in the retina, and is a visual cycle in which photoreceptor optical pigments can maintain the sight and absorb light. It is a retinol isomerase enzyme of RPE involved in important steps. CRALBP is a 36 kDa soluble protein found in the retina that transports the physiological ligand 11-cis-retinol or 11-cis-retinaldehyde. NPR-A regulates gene expression associated with RPE cell proliferation or retinal fluid uptake. RPE65, NPR-A, and CRALBP gene expression were observed to be higher in the 20s SF/P hydrogel compared to 20s and 30s SF and 30 s SF/P hydrogels (**Figures 4B,D**). On day 3, the gene expression profile was observed to be the 20s and 30s SF hydrogel compared with the 20s and 30s SF/P hydrogels for all the marker genes. While the marker gene expression were observed to be significantly increased on day 7 in the 20s and 30s SF/P hydrogels. The expression of the marker gene in the fold was in the order of CRALB > RPE65 > NPR-A as a result. The obtained results clearly infer that the 20s SF/P hydrogel was biocompatible and helps in RPE cell adhesion and proliferation and it was also confirmed that RPE cell proliferation was inhibited when the sonication time exceeds a certain level here it was 20s. This is in agreement with the MTT assay results as mentioned above, confirming that RPE cell proliferation is actively progressing in the 20s SF/P hydrogel.

CONCLUSION

In this study, the 20s and 30s SF and SF/P hydrogels were prepared by sonication for a period of 20s and 30s, respectively. The 20s sonicated SF7P hydrogel sample can be used for transplantation of retinal pigment epithelial cell regeneration. The prepared SF/P hydrogel was observed to have smaller porosity depending on their sonication time and the presence of PEG concentration. It was also confirmed that the compression strength of SF hydrogels without PEG decreases with decreasing sonication time. In addition, FT-IR confirmed that there were no observed changes in the intrinsic components and functional group changes of SF, SF/P, and PEG. The MTT and nuclear stain results confirmed that the cell proliferation rate was higher in the 20s SF/P hydrogel compared with SF seeded cells. Also, the RPE marker gene expression of RPE65, NPRA, and CRALBP, were found to be expressed in higher amounts in the 20s SF/P hydrogel

than that of the other groups (30s SF and SF/P hydrogels). Based on the obtained results of this study, 20s SF/P hydrogel has a positive effect on the proliferation of RPE cells compared with the 30s SF and SF/P hydrogels. Thus, 20s SF/PEG hydrogel can be used as an alternative material in the tissue engineering field, especially for retinal regeneration applications.

DATA AVAILABILITY STATEMENT

The datasets generated for this study are available on request to the corresponding author.

ETHICS STATEMENT

All the animal experiments were performed in accordance with the guidelines and the approval of the Chonbuk National University Animal Care Committee (CBNUACC), Jeonju, South Korea. The protocol was approved by the (CBNUACC).

AUTHOR CONTRIBUTIONS

YJ and HK performed the experiments and wrote the manuscript. MT designed the experiments and wrote the manuscript. MC, GL, CS, and JS performed the *in vitro* studies. GK designed the experiments and proofread the manuscript. All authors contributed to the article and approved the submitted version.

FUNDING

This research was supported by the Basic Science Research Program through the National Research Foundation of Korea (NRF) funded by the Ministry of Science, ICT and Future Planning (NRF-2017R1A2B3010270).

REFERENCES

Algvere, P. V., Berglin, L., Gouras, P., Sheng, Y. H., and Kopp, E. D. (1997). Transplantation of RPE in age-related macular degeneration: observations in disciform lesions and dry RPE atrophy. *Graefes Arch. Clin. Exp. Ophthalmol.* 235, 149–158. doi: 10.1007/Bf00941722

Bhutto, I., and Lutty, G. (2012). Understanding age-related macular degeneration (AMD): relationships between the photoreceptor/retinal pigment epithelium/Bruch's membrane/choriocapillaris complex. *Mol. Aspects Med.* 33, 295–317. doi: 10.1016/j.mam.2012.04.005

Binder, S. (2011). Scaffolds for retinal pigment epithelium (RPE) replacement therapy. *Br. J. Ophthalmol.* 95, 441–442. doi: 10.1136/bjo.2009.171926

Bok, D. (1993). The retinal-pigment epithelium - a versatile partner in vision. *J. Cell Sci.* 17, 189–195. doi: 10.1242/jcs.1993.supplement_17.27

Bressler, N. M., Bressler, S. B., and Fine, S. L. (1988). Age-related macular degeneration. *Survey Ophthalmol.* 32, 375–413. doi: 10.1016/0039-6257(88)90052-5

Chanasakulniyom, M., Glidle, A., and Cooper, J. M. (2015). Cell proliferation and migration inside single cell arrays. *Lab Chip* 15, 208–215. doi: 10.1039/c4lc00774c

Chao, P. H. G., Yodmuang, S., Wang, X. Q., Sun, L., Kaplan, D. L., Vunjak-Novakovic, G., et al. (2010). Silk hydrogel for cartilage tissue engineering. *J. Biomed. Mater. Res. Part B Appl. Biomater.* 95, 84–90. doi: 10.1002/jbm.b.31686

Hageman, G. S., Luthert, P. J., Chong, N. H. V., Johnson, L. V., Anderson, D. H., and Mullins, R. F. (2001). An integrated hypothesis that considers drusen as biomarkers of immune-mediated processes at the RPE-Bruch's membrane interface in aging and age-related macular degeneration. *Prog. Retinal Eye Res.* 20, 705–732. doi: 10.1016/S1350-9462(01)00010-6

Hallab, N. J., Bundy, K. J., O'Connor, K., Moses, R. L., and Jacobs, J. J. (2001). Evaluation of metallic and polymeric biomaterial surface energy and surface roughness characteristics for directed cell adhesion. *Tissue Eng.* 7, 55–71. doi: 10.1089/107632700300003297

Kim, H. S., Kim, D., Jeong, Y. W., Choi, M. J., Lee, G. W., Thangavelu, M., et al. (2019). Engineering retinal pigment epithelial cells regeneration for transplantation in regenerative medicine using PEG/Gellan gum hydrogels. *Int. J. Biol. Macromol.* 130, 220–228. doi: 10.1016/j.jbiomac.2019.01.078

Lee, G. Y., Kang, S. J., Lee, S. J., Song, J. E., Joo, C. K., Lee, D., et al. (2017). Effects of small intestinal submucosa content on the adhesion and proliferation of retinal pigment epithelial cells on SIS-PLGA films. *J. Tissue Eng. Regenera. Med.* 11, 99–108. doi: 10.1002/term.1882

Li, R. H., Altreuter, D. H., and Gentile, F. T. (1996). Transport characterization of hydrogel matrices for cell encapsulation. *Biotechnol. Bioeng.* 50, 365–373. doi: 10.1002/(Sici)1097-0290(19960520)50:4<365::Aid-Bit3>3.0.Co;2-J

Liang, F. Q., and Godley, B. F. (2003). Oxidative stress-induced mitochondrial DNA damage in human retinal pigment epithelial cells: a possible mechanism for RPE aging and age-related macular degeneration. *Exp. Eye Res.* 76, 397–403. doi: 10.1016/S0014-4835(03)00023-X

Liao, J. L., Yu, J. H., Huang, K., Hu, J., Diemer, T., Ma, Z. C., et al. (2010). Molecular signature of primary retinal pigment epithelium and stem-cell-derived RPE cells. *Hum. Mol. Genet.* 19, 4229–4238. doi: 10.1093/hmg/ddq34.1

Lu, B., Malcuit, C., Wang, S. M., Girman, S., Francis, P., Lemieux, L., et al. (2009). Long-term safety and function of RPE from human embryonic stem cells in preclinical models of macular degeneration. *Stem Cells* 27, 2126–2135. doi: 10.1002/stem.149

Lu, Q. A., Zhang, B., Li, M. Z., Zuo, B. Q., Kapan, D. L., Huang, Y. L., et al. (2011). Degradation mechanism and control of silk fibroin. *Biomacromolecules* 12, 1080–1086. doi: 10.1021/bm101422j

Mandelcorn, M. S., Machemer, R., Fineberg, E., and Hersch, S. B. (1975). Proliferation and metaplasia of intravitreal retinal-pigment epithelium cell autotransplants. *Am. J. Ophthalmol.* 80, 227–237. doi: 10.1016/0002-9394(75)90137-3

Ohno, K., Mandai, Y., and Matsuura, H. (1992). Vibrational-spectra and molecular-conformation of taurine and its related-compounds. *J. Mol. Struct.* 268, 41–50. doi: 10.1016/0022-2860(92)85058-O

Park, J. H., Shin, E. Y., Shin, M. E., Choi, M. J., Carlomagno, C., Song, J. E., et al. (2018). Enhanced retinal pigment epithelium (RPE) regeneration using curcumin/alginate hydrogels: in vitro evaluation. *Int. J. Biol. Macromol.* 117, 546–552. doi: 10.1016/j.ijbiomac.2018.05.127

Samal, S. K., Kaplan, D. L., and Chiellini, E. (2013). Ultrasound sonication effects on silk fibroin protein. *Macromol. Mater. Eng.* 298, 1201–1208. doi: 10.1002/mame.201200377

Santin, M., Motta, A., Freddi, G., and Cannas, M. (1999). In vitro evaluation of the inflammatory potential of the silk fibroin. *J. Biomed. Mater. Res.* 46, 382–389. doi: 10.1002/(Sici)1097-4636(19990905)46:3<382::Aid-Jbm11>3.0.Co;2-R

Shin, E. Y., Park, J. H., Shin, M. E., Song, J. E., Thangavelu, M., Carlomagno, C., et al. (2019). Injectable taurine-loaded alginate hydrogels for retinal pigment epithelium (RPE) regeneration. *Mater. Sci. Eng. C Mater. Biol. Appl.* 103:109787. doi: 10.1016/j.msec.2019.109787

Simo, R., Villarroel, M., Corraliza, L., Hernandez, C., and Garcia-Ramirez, M. (2010). The retinal pigment epithelium: something more than a constituent of the blood-retinal barrier-implications for the pathogenesis of diabetic retinopathy. *J. Biomed. Biotechnol.* 2010:15. doi: 10.1155/2010/190724

Strauss, O. (2005). The retinal pigment epithelium in visual function. *Physiol. Rev.* 85, 845–881. doi: 10.1152/physrev.00021.2004

Strauss, O. (2009). The role of retinal pigment epithelium in visual functions. *Ophthalmologe* 106, 299–304. doi: 10.1007/s00347-008-1869-x

Sung, H. J., Meredith, C., Johnson, C., and Galis, Z. S. (2004). The effect of scaffold degradation rate on three-dimensional cell growth and angiogenesis. *Biomaterials* 25, 5735–5742. doi: 10.1016/j.biomaterials.2004.01.066

Vepari, C., and Kaplan, D. L. (2007). Silk as a biomaterial. *Prog. Polym. Sci.* 32, 991–1007. doi: 10.1016/j.progpolymsci.2007.05.013

Wang, K., and Han, Z. C. (2017). Injectable hydrogels for ophthalmic applications. *J. Control. Release* 268, 212–224. doi: 10.1016/j.jconrel.2017.10.031

Wang, X. Q., Kluge, J. A., Leisk, G. G., and Kaplan, D. L. (2008). Sonication-induced gelation of silk fibroin for cell encapsulation. *Biomaterials* 29, 1054–1064. doi: 10.1016/j.biomaterials.2007.11.003

Yucel, T., Cebe, P., and Kaplan, D. L. (2009). Vortex-induced injectable silk fibroin hydrogels. *Biophys. J.* 97, 2044–2050. doi: 10.1016/j.bpj.2009.07.028

Zustiak, S. P., and Leach, J. B. (2010). Hydrolytically degradable poly(Ethylene Glycol) hydrogel scaffolds with tunable degradation and mechanical properties. *Biomacromolecules* 11, 1348–1357. doi: 10.1021/bm100137q

Conflict of Interest: The authors declare that the research was conducted in the absence of any commercial or financial relationships that could be construed as a potential conflict of interest.